Title

Usefulness of three-dimensional magnetic resonance cholangiopancreatography with partial maximum intensity projection for diagnosing autoimmune pancreatitis

Shin Yanagisawa [a]

Yasunari Fujinaga [a]

Takayuki Watanabe [b]

Masahiro Maruyama [b]

Takashi Muraki [b]

Masaaki Takahashi [a]

Akira Fujita [a]

Sachie Fujita [a]

Masahiro Kurozumi [a]

Kazuhiko Ueda [a]

Hideaki Hamano [c]

Shigeyuki Kawa [d]

Masumi Kadoya [a]

[a] Department of Radiology, Shinshu University School of Medicine

3-1-1 Asahi, Matsumoto, 390-8621, Japan

[b] Department of Gastroenterology, Shinshu University School of Medicine

3-1-1 Asahi, Matsumoto, 390-8621, Japan

[c] Department of Medical informatics, Gastroenterology, Shinshu University School of Medicine

3-1-1 Asahi, Matsumoto, 390-8621, Japan

[d] Center for Health, Safety, and Environmental Management, Shinshu University

3-1-1 Asahi, Matsumoto, 390-8621, Japan

Corresponding author: Shin Yanagisawa

Mailing address: Department of Radiology, Shinshu University School of Medicine, 3-1-1 Asahi, Matsumoto, 390-8621, Japan

Tel: +81-263-37-2650

Fax: +81-263-37-3087

E-mail address: shiny@shinshu-u.ac.jp

Abstract

Purpose: To compare three-dimensional magnetic resonance cholangiopancreatography (MRCP) with/without partial maximum intensity projection (MIP) and endoscopic retrograde cholangiopancreatography (ERCP) in patients with autoimmune pancreatitis (AIP).

Materials and Methods: Three-dimensional MRCP and ERCP images were retrospectively analyzed in 24 patients with AIP. We evaluated the narrowing length of the main pancreatic duct (NR-MPD), multiple skipped MPD narrowing (SK-MPD), and side branches arising from the narrowed portion of the MPD (SB-MPD) using four MRCP datasets: 5 original images (MIP_5), 10 original images (MIP_{10}), all original images (full-MIP), and a combination of these three datasets (a-MIP). The images were scored using a 3- or 5-point scale. The scores of the four MRCP datasets were statistically analyzed, and the positive rate of each finding was compared between MRCP and ERCP.

Results: The median scores for SB-MPD on MIP_5 and a-MIP were significantly higher than those on MIP_{10} and full-MIP. In other words, partial MIP is superior to full-MIP for visualization of detailed structures. The positive rate for SB-MPD on full-MIP was significantly lower than that on ERCP, whereas the positive rate on MIP_5, MIP_{10}, and a-MIP was not significantly different from that on ERCP. Moreover, the positive rate for NR-MPD and SK-MPD on the MRCP images was significantly higher than that on the ERCP images.

Conclusion: Partial MIP is useful for evaluating the MPD and is comparable with ERCP for diagnosing AIP.

Introduction

Autoimmune pancreatitis (AIP), characterized by autoimmune processes, was originally described as an unusual type of chronic pancreatitis with diffuse irregular narrowing of the entire main pancreatic duct (MPD) on endoscopic retrograde cholangiopancreatography (ERCP) [1]. ERCP findings diagnostic of AIP include involvement of >1/3 of the MPD, multiple strictures without marked upstream dilatation, and segmental/focal narrowing without marked upstream dilatation [2-8]. These characteristics have been adopted as part of the International Consensus Diagnostic Criteria (ICDC) for Autoimmune Pancreatitis [9]. Secondary pancreatic duct derivation from the narrowed pancreatic duct is also useful in differentiating AIP from pancreatic cancer [10,11].

Magnetic resonance cholangiopancreatography (MRCP), a noninvasive method of evaluating the pancreatic duct, is reportedly useful in diagnosing AIP [12-14]. Some studies, however, have reported that MRCP is suboptimal for the diagnosis of AIP. Because MRCP shows lower resolution than ERCP, MRCP is less able to show detailed strictures and side branches [15,16].

Traditional three-dimensional (3D) MRCP, which requires use of the breath-hold technique to assess the pancreaticobiliary ducts [17,18], is dependent on the patient's respiratory motion, which sometimes causes motion artifacts. Barish et al. [19] performed the first 3D MRCP with the respiratory triggering technique during free breathing. In addition, Papanikolaou et al. [20] reported that 3D MRCP performed with the respiratory triggering technique resulted in a higher contrast-to-noise ratio (CNR) of

the bile duct and MPD than that performed with the breath-hold technique. However, respiratory triggering, which involves monitoring movement of the abdominal wall, does not always reflect the movement of the visceral organs. The navigator-echo triggering technique, which is used to monitor movement of the right diaphragm with navigator echo, was recently reported to show greater spatial resolution and better visualization of the pancreatic and bile ducts than free-breathing 3D MRCP or 2D MRCP [21-23]. In addition, 3D MRCP at 3T resulted in an improved CNR and better visualization than 3D MRCP at 1.5T [24]. However, 3D MRCP has potential drawbacks because it is always displayed using a reconstruction algorithm of maximum intensity projection (MIP). MIP images may be unable to reveal detailed structures because of overlapping bright voxels. Partial MIP, in which the projection volume is limited, may be useful in evaluating specific structures [25]. To our knowledge, no studies have reported differences between 3D MRCP with partial MIP and conventional 3D MRCP. This study was therefore designed to evaluate the usefulness of 3D MRCP with partial MIP in the diagnosis of AIP and to compare 3D MRCP with conventional MRCP and ERCP.

Materials and Methods

This study was approved by the institutional review board of our institution, which waived the requirement for informed consent because of the retrospective design of this study.

Patients

The medical database of our hospital was reviewed to identify patients diagnosed with AIP according to the ICDC from August 2007 to October 2012; who underwent imaging examinations, including 3D MRCP at 3T MRI and ERCP; and were not treated prior to MRI and ERCP evaluation. Twenty-four consecutive patients were identified (16 men and 8 women with a mean age of 62 years).

MRI and pulse sequences

All MR images were obtained with a 3T MR system (Trio Tim; Siemens Healthcare, Erlangen, Germany) using standard body array and spine array coils.

The protocol for pancreatic MRI in our institution included axial T2-weighted imaging [half-Fourier acquisition single-shot turbo spin-echo (HASTE) and fat-suppressed fast spin-echo sequence] and axial T1-weighted gradient-echo imaging, followed by MRCP. Dynamic contrast-enhanced T1-weighted images were acquired as needed. MRCP was performed using a 3D Sampling Perfection with Application-optimized Contrasts using different flip angle Evolution (SPACE) with a respiratory-trigger technique and 2D prospective acquisition correction (PACE). The detailed parameters of MRCP are shown in Table 1. The scanning parameters were set to be as alike as possible, but some parameters varied in accordance with the patients' body size and respiratory cycle. All MRCP results were obtained in the coronal oblique plane at angles parallel to the splenic hilum.

Four MRCP datasets were analyzed: partial MIP with 5 original images (slice thickness = 5–7.5 mm) (MIP_5), partial MIP with 10 original images (slice thickness = 10–15 mm) (MIP_{10}), MIP with all original images (slice thickness = 72–90 mm) (full-MIP), and all three data sets (a-MIP). The slice gaps of MIP_5 and MIP_{10} were the same as the slice thickness of the original images (1–1.5 mm).

Image analysis

MR images were assessed using commercial digital imaging and communication in medicine (DICOM) software (EV Insite; PSP Corporation, Tokyo). All images were independently evaluated by two experienced abdominal radiologists who were blinded to the identifiers and clinical information. Findings evaluated included the length of the MPD narrowing (NR-MPD), multiple skipped MPD narrowing (SK-MPD), and side branches arising from the narrowed portion of the MPD (SB-MPD). NR-MPD was scored using a 3-point scale (0, absent; 1, present in <1/3 of the length of the MPD; and 2, present in ≥1/3 of the length of the MPD). SK-MPD and SB-MPD were scored using a 5-point scale (0, definitely absent; 1, probably absent; 2, equivocal; 3, probably present; and 4, definitely present). An NR-MPD score of 2 (MPD narrowing in ≥1/3 of the MPD) and SK-MPD and SB-MPD scores of 4 and 5 were regarded as positive findings. The evaluators assessed each finding based on the four datasets, with a >2-week interval between dataset assessments. Disagreements between the two evaluators were resolved by discussion and consensus.

Two internal medicine physicians assessed the positivity or negatively of NR-MPD, SK-MPD, and SB-MPD on ERCP; these evaluators were blinded to the patients' clinical information.

Statistical analysis

Statistical analyses were performed with a statistical software package (Prism, version 6.01; GraphPad Software, San Diego, CA). The Friedman test was used to compare the scores for each MR finding in the four MRCP datasets. Fisher's exact test was used to compare the positive rate of each finding in each MRCP dataset and ERCP. A *P*-value of <0.05 was defined as statistically significant.

Results

The distribution of scores for NR-MPD, SK-MPD, and SB-MPD on MIP_5, MIP_{10}, full-MIP, and a-MIP are shown in Figure 1. The median scores for NR-MPD and SK-MPD in all four MIP datasets were 2 and 4, respectively. The median scores for SB-MPD on MIP_5, MIP_{10}, full-MIP, and a-MIP were 4, 3, 2, and 4, respectively; they were significantly lower in the full-MIP dataset than in the other three datasets ($P < 0.05$). Typical images are shown Figure 2.

The positivity rates in the MIP_5, MIP_{10}, full-MIP, and a-MIP datasets and ERCP were 0.92, 0.86, 0.83, 0.86, and 0.50, respectively, for NR-MPD; 0.86, 0.75, 0.79, 0.86, and 0.42, respectively, for SK-MPD; and 0.79, 0.86, 0.43, 0.83, and 0.86, respectively, for SB-MPD. The positivity rates for

NR-MPD and SK-MPD were significantly higher in all four MRCP datasets than in ERCP ($P < 0.05$) (Fig. 3). The positivity rate for SB-MPD was significantly lower in the full-MIP dataset than in ERCP ($P < 0.05$), whereas the other three MRCP datasets did not differ significantly from ERCP (Fig. 4).

Discussion

One of the important findings of this study is that the score for SB-MPD was lower in the full-MIP dataset than in the other three MRCP datasets. This finding suggests that partial MIP has advantages in visualizing small branches of the pancreatic duct. On MR angiography, contrast on MIP usually depends on the intensities of the target structures and background. High-quality contrast images have been reported when the signal intensity of the vessel was about two standard deviations above the mean background noise [26]. Thus, the inability of MIP to visualize extremely fine vessels may be due to a low signal-to-noise ratio (SNR). Similarly, the poor visualization of small branches in the full-MIP dataset may have been due to a low SNR resulting from the large numbers of overlapping original images. In addition, many overlapping images in the full-MIP dataset included other structures or organs, such as the bile duct, stomach, duodenum, and kidneys. In contrast, partial MIP could have helped to achieve an accurate diagnosis of AIP in our study. Takuma et al. [27] reported that SB-MPD was a useful finding suggesting AIP; however, this finding was more faintly visualized on MRCP than on ERCP. On the other hand, our study shows that partial MIP is superior to full-MIP and comparable with ERCP in the

visualization of SB-MPD. In other words, the partial MIP used in the present study could allow for clearer visualization of detailed structures (e.g., SB-MPD). In contrast, the scores for NR-MPD and SK-MPD were similar among the four MRCP datasets. Because the diameter of the MPD is usually larger than that of its side branches, the SNR of the MPD is likely maintained on full-MIP.

The recent development of MR techniques with a high CNR has resulted in improved image resolution. 3D MRCP using navigator-echo triggering may better overcome respiratory motion artifacts than the breath-hold technique [21-23]. The former technique is clinically useful in evaluating the abdominal area, which is easily affected by respiratory motions. Visualization of small branches of the pancreatic duct may have also been facilitated by our use of 3T MRI, which results in a two-fold higher SNR than 1.5T MRI, resulting in high-resolution MRCP with thin sections and a small voxel size [24,28]. High-resolution and high-CNR 3D MRCP with partial MIP may improve visualization of small aspects of the pancreaticobiliary system, such as SB-MPD [25].

ERCP is useful in evaluating the bile and pancreatic ducts of patients with malignant lesions and inflammation, such as AIP. This technique has been incorporated into diagnostic and therapeutic procedures for pancreaticobiliary diseases. According to the ICDC, MPD findings are usually obtained using ERCP [9], whereas MRCP is not recommended because of its lower resolution than ERCP. Our results, however, indicate that the image quality of 3D MRCP is comparable with that of ERCP. Moreover, ERCP is an invasive technique requiring cannulation of the biliary and pancreatic ducts and performance

of biopsies, which may result in various complications such as pancreatitis, bleeding, and cholangitis [29-31]. In contrast, MRCP is a noninvasive and safer procedure, suggesting that 3D MRCP findings may useful in the diagnosis of AIP.

Interestingly, we found that the positivity rates of NR-MPD and SK-MPD were significantly higher in MRCP than ERCP. Using contrast medium in the MPD, ERCP can directly distinguish the ducts and show their shapes. In contrast, MRCP is performed without putting pressure on the MPD. The diameter of the MPD was found to be larger on ERCP than on MRCP in patients with chronic pancreatitis, perhaps because the use of contrast medium in ERCP results in distention of the MPD; thus, ERCP may overestimate its diameter [32]. The diameter of the MPD on MRCP appears to reflect the physiological flow of bile and pancreatic fluid; therefore, ERCP may underestimate some MPD findings relative to MRCP. In contrast, no discrepancies between MRCP and ERCP findings have been reported in patients with pancreatic cancer. Therefore, it is necessary to determine whether discrepancies between MRCP and ERCP findings are useful in differentiating focal AIP from pancreatic cancer.

This study had several limitations, including its retrospective design and inclusion of a small number of patients. Prospective studies with large numbers of patients may be necessary to validate our results. Second, there was no gold standard for the MPD findings. Although our findings suggested that ERCP may underestimate the MPD findings compared with MRCP, the true condition could not be established, especially in patients with benign lesions (e.g., AIP). Carbognin et al. [33] showed that

secretin-enhanced MRCP was a useful method in the differential diagnosis between focal AIP and pancreatic carcinoma. This method could show more physiological pancreatic secretion than ERCP with contrast medium. Unfortunately, secretin is not approved for the diagnosis of AIP in Japan; however, this method could help to resolve the discrepancy between the ERCP and MRCP findings.

Conclusion

MRCP is comparable with ERCP for diagnosing AIP. In addition, partial MIP is useful for evaluating the pancreatic duct, especially small branches from the MPD.

References

1. Toki F, Kozu T, Oi I, Nakasato T, Suzuki M, Hanyu F. An unusual type of chronic pancreatitis showing diffuse irregular narrowing of the entire main pancreatic duct on ERCP—a report of four cases [abstract]. Endoscopy 1992;24:640.
2. Horiuchi A, Kawa S, Akamatsu T, Aoki Y, Mukawa K, Furuya N, et al. Characteristic pancreatic duct appearance in autoimmune chronic pancreatitis: a case report and review of the Japanese literature. Am J Gastroenterol 1998;93:260–3.
3. Horiuchi A, Kawa S, Hamano H, Hayama M, Ota H, Kiyosawa K. ERCP features in 27 patients

with autoimmune pancreatitis. Gastrointest Endosc 2002;55:494–9.

4. Yoshida K, Toki F, Takeuchi T, Watanabe S, Shiratori K, Hayashi N. Chronic pancreatitis caused by an autoimmune abnormality. Proposal of the concept of autoimmune pancreatitis. Dig Dis Sci 1995;49:1561–8.

5. Wakabayashi T, Kawaura Y, Satomura Y, Watanabe S, Shiratori K, Hayashi N. Clinical and imaging features of autoimmune pancreatitis with focal pancreatic swelling or mass formation: comparison with so-called tumor-forming pancreatitis and pancreatic carcinoma. Am J Gastroenterol 2003;98:2679–87.

6. Nakazawa T, Ohara H, Sano H, Ando T, Imai H, Takeda H, et al. Difficulty in diagnosing autoimmune pancreatitis by imaging findings. Gastrointest Endosc 2007;65:99–108.

7. Nishino T, Oyama H, Toki F, Shiratori K. Differentiation between autoimmune pancreatitis and pancreatic carcinoma based on endoscopic retrograde cholangiopancreatography findings. J Gastroenterol 2010;45:988–96.

8. Kamisawa T, Imai M, Chen PY, Tu Y, Egawa N, Tsuruta K, et al. Strategy for differentiating autoimmune pancreatitis from pancreatic cancer. Pancreas 2008;37:e62–7.

9. Shimosegawa T, Chari ST, Frulloni L, Kamisawa T, Kawa S, Mino-Kenudson M, et al. International Association of Pancreatology, International consensus diagnostic criteria for autoimmune pancreatitis: guidelines of the International Association of Pancreatology. Pancreas

2011;40:352–8.

10. Kamisawa T, Okazaki K, Kawa S, Ito T, Inui K, Irie H, et al. Working Committee of the Japan Pancreas Society and the Research Committee for Intractable Pancreatic Disease supported by the Ministry of Health, Labour and Welfare of Japan, Amendment of the Japanese Consensus Guidelines for Autoimmune Pancreatitis, 2013 III. Treatment and prognosis of autoimmune pancreatitis. J Gastroenterol 2014;49:961–70.

11. Kawa S, Okazaki K, Kamisawa T, Kubo K, Ohara H, Hasebe O, et al. Working Committee of the Japan Pancreas Society and the Research Committee for Intractable Pancreatic Disease supported by the Ministry of Health, Labour and Welfare of Japan, Amendment of the Japanese Consensus Guidelines for Autoimmune Pancreatitis, 2013 II. Extrapancreatic lesions, differential diagnosis. J Gastroenterol 2014;49:765–84.

12. Frulloni L, Scattolini C, Falconi M, Zamboni G, Capelli P, Manfredi R, et al. Autoimmune pancreatitis: differences between the focal and diffuse forms in 87 patients. Am J Gastroenterol 2009;104:2288–94.

13. Kamisawa T, Chen PY, Tu Y, Nakajima H, Egawa N, Tsuruta K, et al. MRCP and MRI findings in 9 patients with autoimmune pancreatitis. World J Gastroenterol 2006;12:2919–22.

14. Negrelli R, Manfredi R, Pedrinolla B, Boninsegna E, Ventriglia A, Mehrabi S, et al. Pancreatic duct abnormalities in focal autoimmune pancreatitis: MR/MRCP imaging findings. Eur Radiol

2015;25:359–67.

15. Kamisawa T, Tu Y, Egawa N, Tsuruta K, Okamoto A, Kodama M, et al. Can MRCP replace ERCP for the diagnosis of autoimmune pancreatitis? Abdom Imaging 2009;34:381–4.

16. Park SH, Kim MH, Kim SY, Kim HJ, Moon SH, Lee SS, et al. Magnetic resonance cholangiopancreatography for the diagnostic evaluation of autoimmune pancreatitis. Pancreas 2010;39:1191–8.

17. Takehara Y, Ichijo K, Tooyama N, Kodaira N, Yamamoto H, Tatami M, et al. Breath-hold MR cholangiopancreatography with a long-echo-train fast spin-echo sequence and a surface coil in chronic pancreatitis. Radiology 1994;192:73–8.

18. Lee MG, Lee HJ, Kim MH, Kang EM, Kim YH, Lee Sg, et al. Extrahepatic biliary disease: 3D MR cholangiopancreatography compared with endoscopic retrograde cholangiopancreatography. Radiology 1997;202:663–9.

19. Barish MA, Yucel EK, Soto JA, Chuttani R, Ferrucci JT. MR cholangiopancreatography: Efficacy of three-dimensional turbo spin-echo technique. AJR Am J Roentgenol 1995;165:295–300.

20. Papanikolaou N, Karantanas AH, Heracleous E, Costa JC, Gourtsoyiannis N. Magnetic resonance cholangiopancreatography: Comparison between respiratory-triggered turbo spin echo and breath hold single-shot turbo spin echo sequences. Magn Reson Imaging 1999;17:1255–60.

21. Morita S, Ueno E, Suzuki K, Machida H, Fujimura M, Kojima S, et al. Navigator-triggered

prospective acquisition correction (PACE) technique vs. conventional respiratory-triggered technique for free-breathing 3D MRCP: an initial prospective comparative study using healthy volunteers. J Magn Reson Imaging 2008;28:673–7.

22. Asbach P, Klessen C, Kroencke TJ, Kluner C, Stemmer A, Hamm B, et al. Magnetic resonance cholangiopancreatography using a free-breathing T2-weighted turbo spin-echo sequence with navigator-triggered prospective acquisition correction. Magn Reson Imaging 2005;23: 939–45.

23. Matsunaga K, Ogasawara G, Tsukano M, Iwadate Y, Inoue Y. Usefulness of the navigator-echo triggering technique for free-breathing three-dimensional magnetic resonance cholangiopancreatography. Magn Reson Imaging 2013;31:396–400.

24. Merkle EM, Haugan PA, Thomas J, Jaffe TA, Gullotto C. 3.0- Versus 1.5-T MR cholangiography: a pilot study. AJR Am J Roentgenol 2006;186:516–21.

25. Leyendecker JR, Rivera E Jr, Washburn WK, Johnson SP, Diffin DC, Eason JD. MR angiography of the portal venous system: techniques, interpretation, and clinical applications. Radiographics 1997;17:1425–43.

26. Anderson CM, Saloner D, Tsuruda JS, Shapeero LG, Lee RE. Artifacts in maximum-intensity-projection display of MR angiograms. AJR Am J Roentgenol 1990;154:623–9.

27. Takuma K, Kamisawa T, Tabata T, Inaba Y, Egawa N, Igarashi Y. Utility of pancreatography for

diagnosing autoimmune pancreatitis. World J Gastroenterol 2011;17:2332–7.

28. Isoda H, Kataoka M, Maetani Y, Kido A, Umeoka S, Tamai K, et al. MRCP imaging at 3.0 T vs. 1.5 T: preliminary experience in healthy volunteers. J Magn Reson Imaging 2007;25:1000–6.

29. Freeman ML, DiSario JA, Nelson DB, Fennerty MB, Lee JB, Bjorkman DJ, et al. Risk factors for post-ERCP pancreatitis: a prospective, multicenter study. Gastrointest Endosc 2001;54:425–34.

30. Vandervoort J, Soetikno RM, Tham TC, et al. Risk factors for complications after performance of ERCP. Gastrointest Endosc 2002;56:652–6.

31. Cheng CL, Sherman S, Watkins JL, Barnett J, Freeman M, Geenen J, et al. Risk factors for post-ERCP pancreatitis: a prospective multicenter study. Am J Gastroenterol 2006;101:139–47.

32. Tamura R, Ishibashi T, Takahashi S. Chronic pancreatitis: MRCP versus ERCP for quantitative caliber measurement and qualitative evaluation. Radiology 2006;238:920–8.

33. Carbognin G, Girardi V, Biasiutti C, Camera L, Manfredi R, Frulloni L, et al. Autoimmune pancreatitis: imaging findings on contrast-enhanced MRCP and dynamic secretin-enhanced MRCP. Radiol med 2009;114:1214-31.

Table 1

Sequence parameters of magnetic resonance cholangiopancreatography

Repetition time (TR) (ms)	2983–8853[a]
Echo time (TE) (ms)	601–649
Flip angle factor	Constant[b]
Echo-train duration (ms)	1020
Turbo factor	63
Parallel acquisition technique factor	3
Field of view (mm)	300–320 × 300–320
Acquisition matrix (mm)	320 × 289–309
Slice thickness (mm)	1–1.5
Slice number	60–80
Acquisition time (min)	3–5[c]

[a] TR differed among subjects according to respiratory cycles.

[b] The flip angle evolution in Application optimized Contrasts using different flip angle Evolution (SPACE) was calculated to achieve a high and nearly constant signal of tissues during most of the duration of signal acquisition.

[C] Acquisition time differed among subjects according to respiratory cycle.

Figure 1

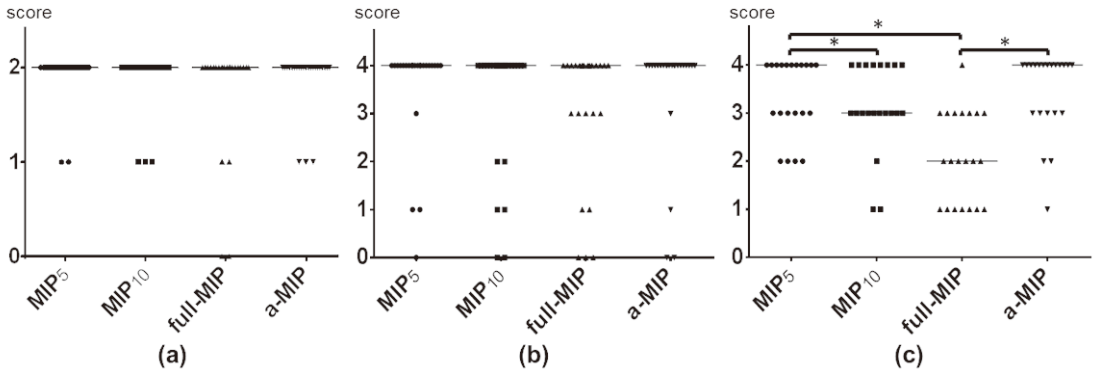

Distribution of scores on magnetic resonance cholangiopancreatography (MRCP). (a) Length of the main pancreatic duct (MPD) narrowing (NR-MPD). (b) Multiple skipped MPD narrowing (SK-MPD). (c) Side branches arising from the narrowed portion of the MPD (SB-MPD). The scores in the four datasets were similar in (a) and (b) but were significantly lower (* $P < 0.05$) for full-MIP than for the other three datasets in (c). Abbreviations: MIP_5, partial maximum intensity projection (MIP) with 5 original images; MIP_{10}, partial MIP with 10 original images; full-MIP, MIP with all original images; a-MIP, all three datasets

Figure 2

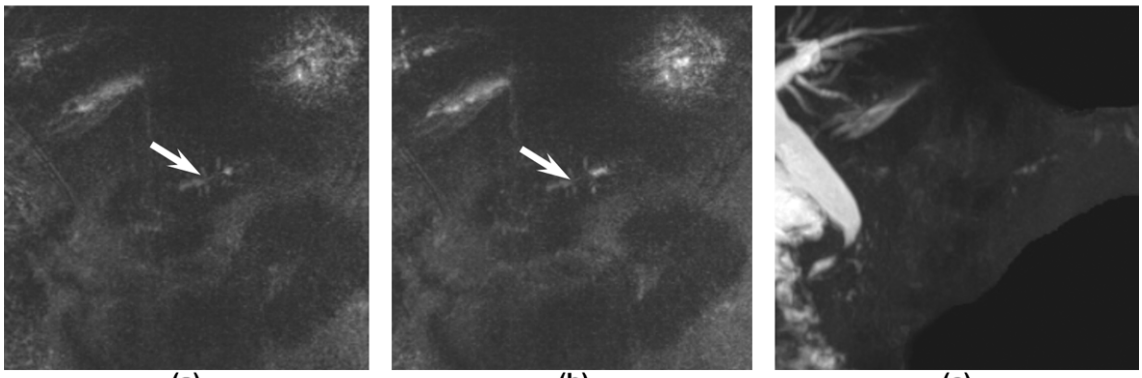

MIP reconstructions obtained from a 69-year-old man with autoimmune pancreatitis. MIP_5 (a) and MIP_{10} (b) clearly showed side branches arising from the narrowed portion of the main pancreatic duct (SB-MPD) (arrow), whereas full-MIP (c) was unclear.

Figure 3

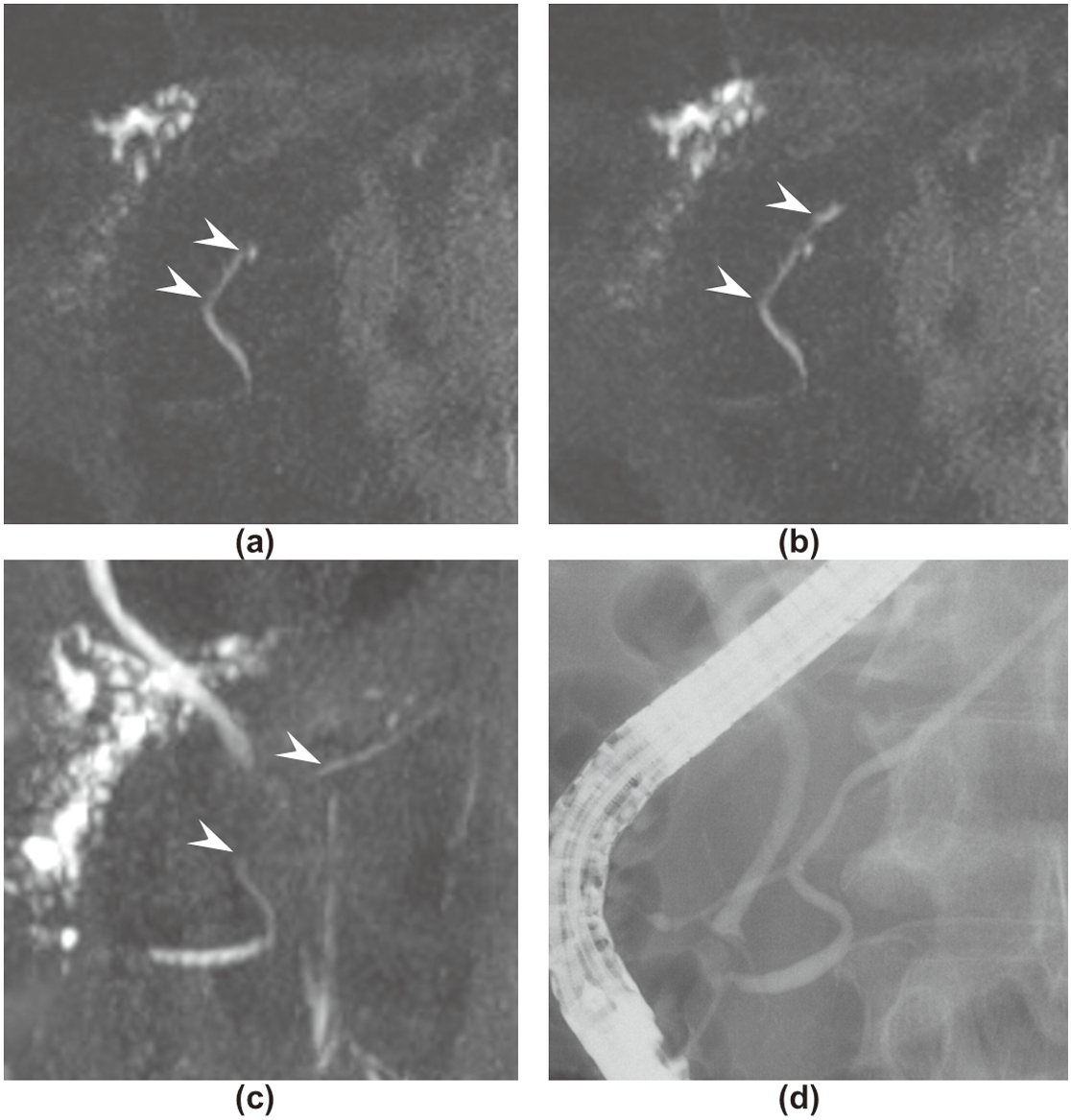

MIP reconstructions and ERCP obtained from a 57-year-old man with autoimmune pancreatitis. MIP_5 (a), MIP_{10} (b) and full-MIP (c) clearly showed the length of the main pancreatic duct narrowing (NR-MPD) (arrow head), whereas ERCP (d) was unclear.

Figure 4

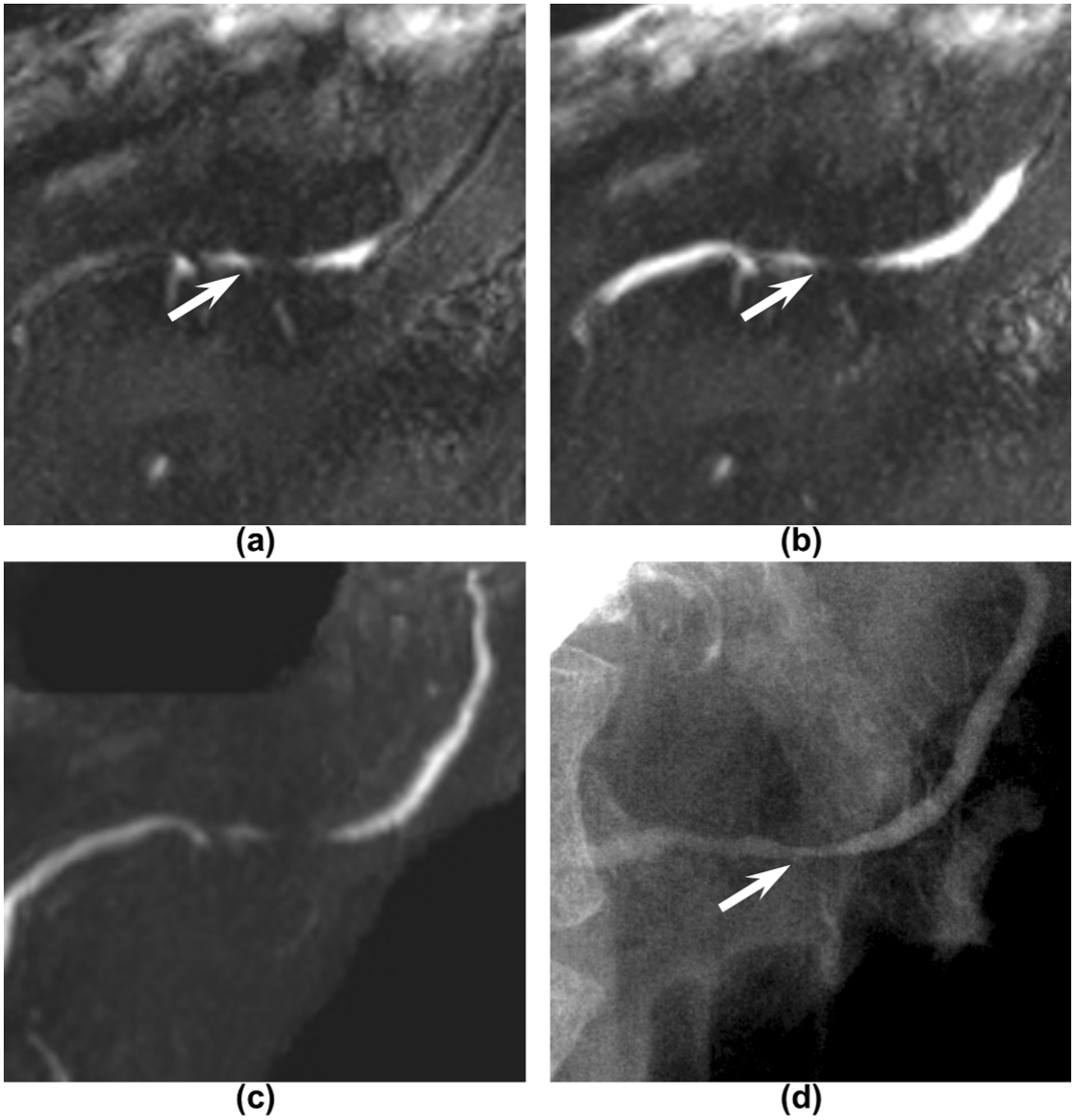

MIP reconstructions and ERCP obtained from a 58-year-old woman with autoimmune pancreatitis. MIP_5 (a) and MIP_{10} (b) clearly showed side branches arising from the narrowed portion of the main pancreatic duct (SB-MPD) (arrow), whereas full-MIP (c) was unclear. The visibilities of SB-MPD on MIP_5 and MIP_{10} were nearly comparable with that of ERCP (arrow) (d).